ATTACHMENT 6

CORE SHROUD BOAT SAMPLE TESTING SUMMARY

Interpretive Metallurgical Report on

Core Shroud Vertical Weld Boat Samples

from Nine Mile Point Unit 1

Technical Report No. 97181-TR-02
Revision 0
Volume 1 of 1

prepared for:

Niagara Mohawk Power Corporation

Nine Mile Point Unit 1

February 1998

a4b

altran

Report Record

Document No.: 97181-TR-02 Rev. No.: 0 Sheet No.: 1

Nuclear Safety Related Yes ___ No X Total No. of Sheets 16

TITLE: Interpretive Metallurgical Report on Core Shroud Vertical Weld Boat Samples from NMP-1

CLIENT: Niagara Mohawk **FACILITY:** NMP - Unit 1

REV. DESCRIPTION: Revision 0 - Original Issue

COMPUTER RUNS (identified on Computer File Index): Yes ___ N/A X

Error reports evaluated by: ____________ Date: ____________

Impacted by error reports: No ___ Yes ___ (if yes, attach explanation)

Originator(s)	Date	Checker(s)	Date
R. E. Smith R.E. Smith	2/24/98 2/24/98		

DESIGN VERIFICATION: (EOP 3.4) Required ___ Not Required* X

* Justification Non "QA"

Performed by: ____________ Date: ____________

Method of design verification:

___ Design Review ___ Alternate Calculations (Attached) ___ Qualification Test (Data/Results Attd.)

Comments resolved by: ____________ Date: ____________

Design verifier concurrence: ____________ Date: ____________

APPROVED FOR RELEASE

PROJECT MANAGER: R. E. Smith Date: 2/24/98
R.E. Smith

ENGINEERING MANAGER: Mary G Addley Date: 2/24/98
for D.S. Williams

TABLE OF CONTENTS

LIST OF FIGURES

Interpretive Metallurgical Report on Core Shroud Vertical Weld Boat Samples from Nine Mile Point Unit 1

1.0 Executive Summary

A metallurgical investigation has been conducted on two boat samples removed from the Nine Mile Point Unit 1 (NMP1) core shroud. This evaluation interprets results from this investigation in light of plant operating conditions. The metallurgical tests were conducted by McDermott Technologies in their hot cell facilities at the Lynchburg Research Center (LRC). The initial results have been reported in an earlier report (Reference 11). Those results and the additional information described in this report provide clear metallurgical evidence suggesting an intergranular stress corrosion cracking (IGSCC) failure mechanism. The findings confirm the mechanistic assumptions of cracking analyses submitted previously to the Nuclear Regulatory Commission (References 1 – 4). The findings are consistent with the mechanistic understanding of IGSCC initiation and growth processes for Boiling Water Reactor (BWR) core shrouds presented in BWRVIP-14. No metallurgical evidence was discovered that supported an irradiation-assisted stress corrosion (IASCC) mechanism.

2.0 Introduction

Crack-like indications were observed on the outer surface along the length of welds V-9 and V-10 using enhanced visual inspection techniques consistent with recommendations developed for the BWROG Vessel Internals Program. Visual indications were confirmed using remote ultrasonic testing methods, and crack depths were determined along the lengths of the vertical welds by measuring from the outer surface using UT sizing methods. The General Electric Company (GE) developed specific equipment for core shroud examinations including the Trimodal Core Shroud search unit, the GE Smart 2000 ultrasonic examination system, and the GE Suction Cup Scanner.

The cracks on the right side of weld V-10 (viewed with the shroud oriented vertically) are reasonably represented by a single continuous crack indication running parallel to the weld. The cracks are essentially bounded within a volume of material adjacent to the weld fusion interface known as the weld heat affected zone (HAZ). Cracking is restricted to the outer surface at this weld. Crack depths typically were measured from 0.4 to 0.7 inches, although several specific locations along the length of this weld were deeper. Figure 1 presents a profile of the depths of cracking along the length of the V-10 weld. In general the cracking was slightly deeper towards the top and shallower towards the bottom. Actual data are discrete measurements plotted as if they were continuous. No cracking was seen immediately adjacent to the horizontal welds bounding the top and bottom of the shell course. Eight short crack segments (parallel to the weld) were seen on the outer surface to the left side of weld V-10 as shown in Figure 2.

Cracking patterns are similar on the outer surface of weld V-9 except that cracking was predominantly on the left side of the weld. Figure 3 presents the depth profile of cracking measured along the length of weld V-9. The maximum depth of cracking associated with the left outer surface of weld V-9 is greater than the maximum depth of cracking associated with weld V-10. It should be noted that the left side of V-9 and the right side of V-10 are the same plate of material. [Note: There were two short crack segments on the right side originating at the inner surface, and these were the only inner surface cracks associated with either of the vertical welds, V-9 and V-10.]

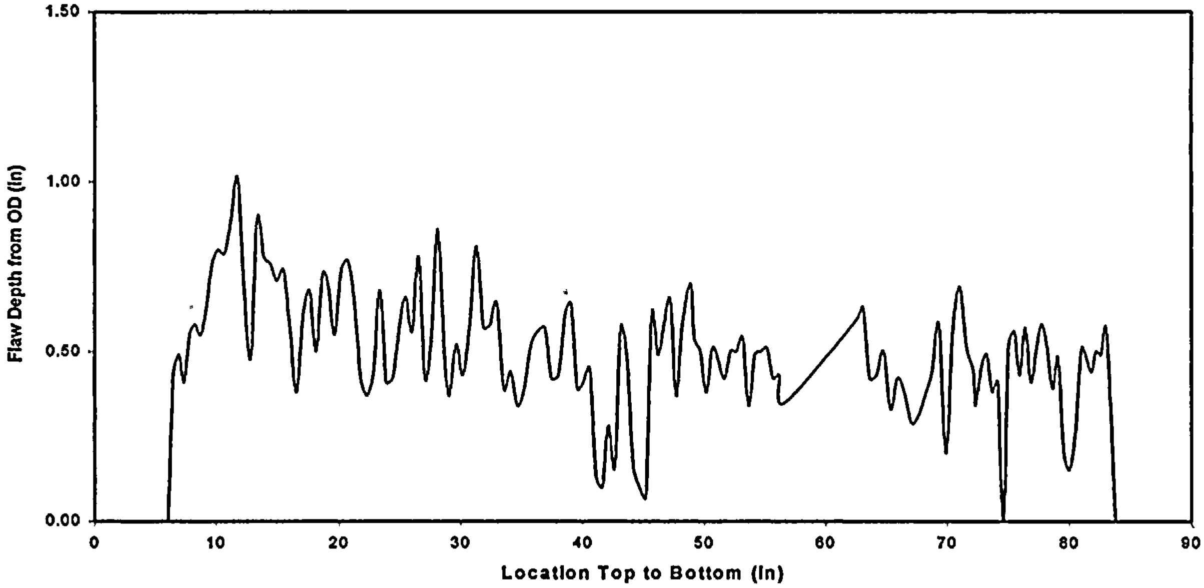

Figure 1 - Crack depth profile for right side of vertical weld V-10

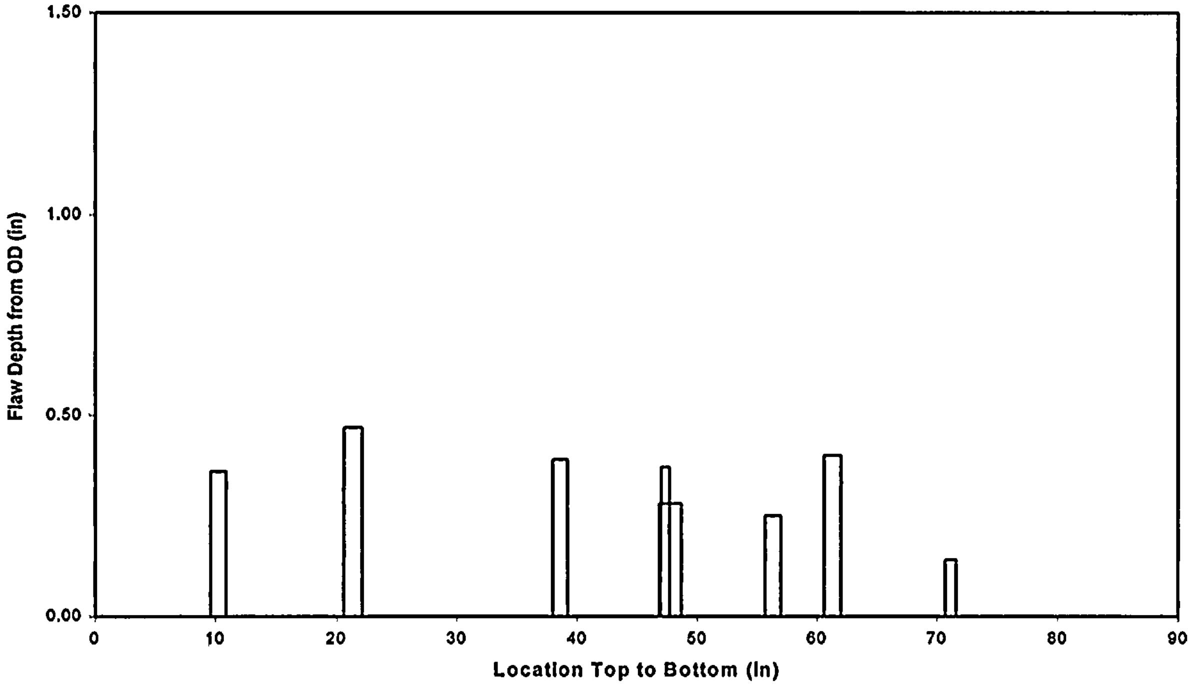

Figure 2 - Crack depth profile for left side of vertical weld V-10

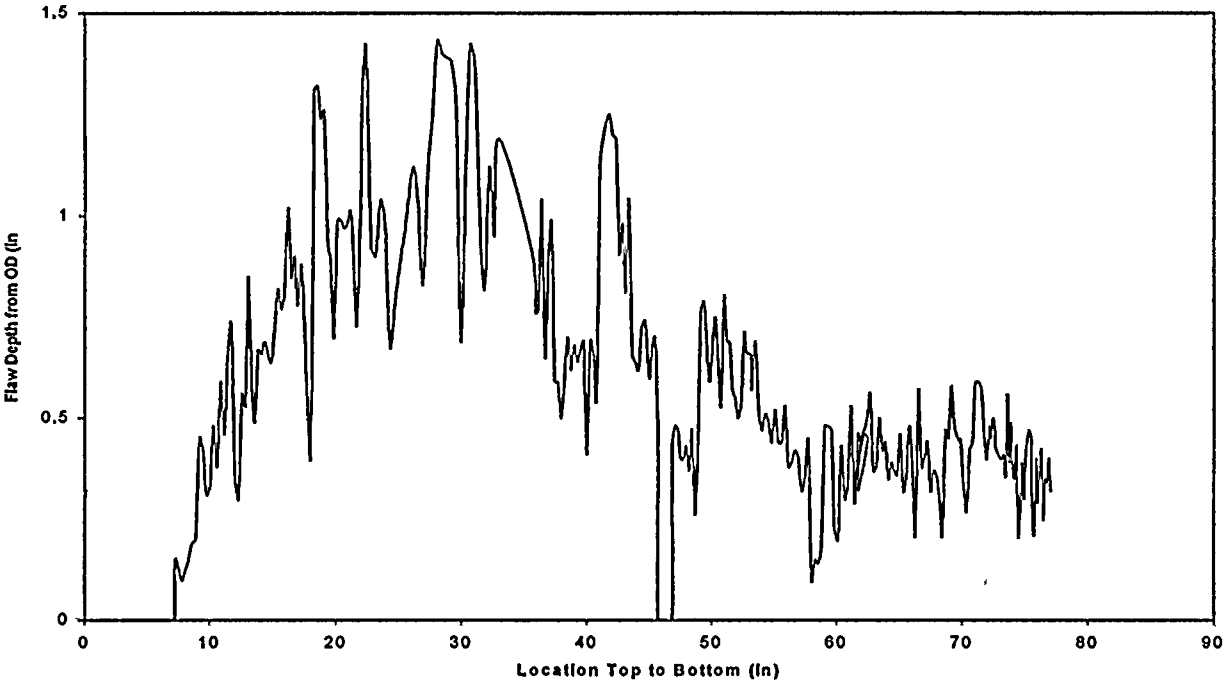

Figure 3 - Crack depth profile for left side of vertical weld V-9

The metallurgical evaluation examined two boat samples taken from the welds designated as V-9 and V-10 that join the plates forming the central-mid-cylinder shell course. This cylinder is located approximately at the core mid-plane. Boat sample V-10 was removed from the outer surface and was positioned such that it contained a sample of the crack having a depth that could be captured within the volume of the boat sample. The EDM sampling cutter was positioned on the outer surface such that the edge of the weld would be located to the left side of the boat sample, and should contain the edge of the weld deposit. The vertical location was approximately 57.5 inches below the upper horizontal weld, H-4. Sample V-10 was used primarily to document representative metallurgical features associated with cracking of the vertical welds. Boat sample V-9 was not cracked, and was removed from the inner surface of the shroud. It was located to the right of weld V-9 at an elevation approximately 25 inches below the upper horizontal weld, H-4. This latter sample represented a high fluence location and was used to determine if the accumulated fluence resulted in measurable materials effects such as degree of sensitization or radiation hardening. The sampling device was positioned in a manner similar to V-10 so that the edge of the weld could be captured. Figure 4 is a sketch that shows the locations from which the boat samples were removed.

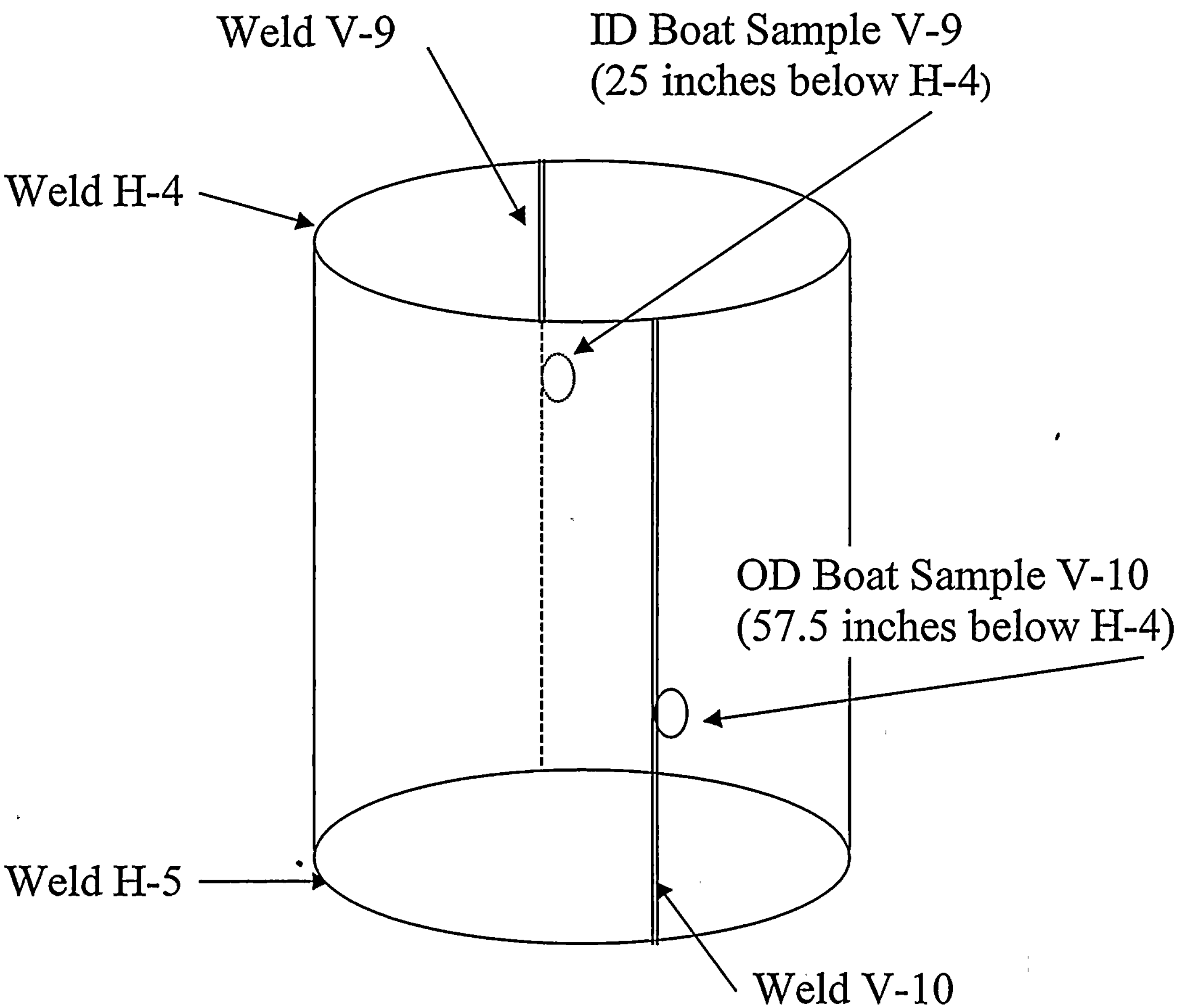

Figure 4 - Sketch of the locations for boat samples V-9 & V-10

The cracking found on the outer surfaces of vertical welds V-9 and V-10, was oriented predominantly parallel to the length of the weld. The extensive cracking associated with the V-9 and V-10 welds was biased toward the plate from which the V-10 boat sample was removed. The modest degree of cracking found in the other plate was shown in Figure 2. The V-9 boat sample was taken from the inner surface of the other plate that makes up the central mid-cylinder section. This selection strategy provided for comparisons between the two heats of material. It should be noted that both plates display susceptibility to cracking, but one plate seemed to have a greater propensity to cracking. Once cracking initiated in either plate, the stress field would be reduced on the other side of the weld because these are localized residual stresses.

3.0 Industry Background

Core shroud cracking experience in Boiling Water Reactors (BWRs) dates back to October 1990, when the initial observation of such cracking was reported in a European BWR. Since that time cracking has been observed in many of the domestic and overseas BWRs reporting inspection results to the BWR industry. The cracking is typically observed in weld HAZs of horizontal (circumferential) and vertical welds within the shell cylinder, and in HAZs of welds joining ring segments. Both Type 304 and Type 304-L stainless steel materials have cracked. In several cases, cracking has been confirmed by destructive metallurgical examination of boat or plug samples removed from the core shroud in the vicinity of the cracking. The cracking experience has extended from the uppermost horizontal weld in the core shroud (the H1 weld), to the core plate support ring weld (the H5 or H6A or H6B) depending upon the specific shroud design. In the case of Nine Mile Point Unit 1, cracking has been identified in the HAZ of the weld joining the core shroud to the beveled shroud support ring.

Cracking is normally contained within the HAZs of structural welds, but in a few cases some cracking was observed in base metal remote from the weld HAZ. The sources of the essential conditions for IGSCC included fabrication or installation processes that resulted in localized surface areas being welded or ground. Temporary attachments for support structures or adjusting hardware and cosmetic surface repairs represent a majority of such conditions. Cracking found associated with these localized areas is normally limited to a small size because the local surface areas having the requisite conditions for cracking are limited in size. Welding processes produce both metallurgical structures that are susceptible to IGSCC and high tensile residual stress fields. The tensile stress fields are required to provide driving energy for crack propagation. At least one plant has reported cracking in the weld metal.

4.0 Core Shroud General Description

The core shroud geometry at Nine Mile Point Unit 1 (NMP-1) is that of a stepped right cylinder. The structure is larger at the top in order to accommodate the core spray piping and nozzles without interfering with the direct vertical movement of fuel elements. The cylinder steps inward to the core plate diameter at the Top Guide elevation. Other core shrouds have different geometries. NMP-1 is a BWR Model 2 having five recirculation piping loops (external pumps). The core shroud structure below the core plate is welded to a beveled ring support. The beveled support ring is attached directly to the reactor pressure vessel wall and supports the weight of the shroud and other components supported by the shroud. The ring support geometry is that of a conical shell welded directly to the pressure vessel.

The core shroud functions to direct the flow of cooling water upward through the core and through the steam separator tubes located in the separator head. Note the separator head is bolted directly to the top of the upper core shroud flange and separates the core shroud from the upper plenum. The upper plenum is the volume in which the water separated from the steam is mixed with the makeup feedwater and begins its downward recirculation flow through the annulus volume between the outer surface of the core shroud and the reactor pressure vessel wall.

The water in the lower portion of the annulus is drawn through the suction nozzles of each of the external recirculation pumps. These pumps deliver the coolant back to the reactor vessel at a location below the conical support ring and into the lower plenum. This action directs the flow back to the reactor core to complete the circuit.

The core shroud at NMP-1 is not designed to provide reflood capability during a hypothetical loss of coolant accident (LOCA). NMP-1 is a BWR 2 design and post-LOCA core cooling is provided by the core spray system.

The NMP-1 core shroud is fabricated from a number of individual type 304 stainless steel plates of 1½ inch thickness. Specific fabrication effects are discussed in Reference 3. The sequence with which the shroud is fabricated, and the welding of the individual plates to form cylindrical components, can develop large complex residual stress fields. These are the stress fields known to provide the driving energy for stress corrosion cracking in core shroud weldments.

5.0 Analysis

A metallurgical investigation was conducted on the two boat samples removed from the NMP1 core shroud. The purposes of the investigation were to confirm that IGSCC was the mechanism for cracking, to determine if irradiation assisted stress corrosion mechanisms were involved, and to validate the crack depth measurements. The following tasks were accomplished:

- Receipt of photographic documentation of both boat samples shipped from the site
- Sectioning the boat samples for examination of both cracked and uncracked locations,
- Documentation of microstructural features of both samples,
- Evaluation of individual cracking morphologies and patterns,
- Microhardness measurement profiles at selected locations,
- Chemical analyses of boat samples,
- Examination of oxides present on crack surfaces,
- Documentation of microstructural evidence for sensitization in each sample,
- Measurement of electrochemical potentiokinetic reactivation (EPR) test results for both boat samples,
- Measurement of the neutron fluence with energies above 1 Mev for the V-9 and V-10 boat samples, and
- Tensile tests of the V-9 and V-10 boat sample material.

The remaining planned testing of the boat sample material is the fracture toughness associated with the highest fluence sample. The feasibility studies for completing this testing is in progress.

The following key observations are made from the results of the metallurgical investigation of the boat samples removed from the core shroud at NMP-1, and are detailed in the following eight general areas.

5.1 Nature of Cracking

- All primary and secondary cracking is intergranular.
- The primary crack initiates on the surface and propagates approximately 0.4 inch in depth. This depth is consistent with ultrasonic depth measurements adjacent to the sampling location.
- Multiple primary cracks initiate on the specimen surface (likely branched from the main trunk).
- The primary crack has fractured oxides on crack faces.
- Some secondary cracks propagate approximately perpendicular to the weld fusion line and initiate subsurface.
- Secondary cracks are completely filled with oxides. This characteristic is consistent with a stationary or non-growing crack.
- Grain encirclement is associated with the primary crack.
- Oxides are observed near the crack tip.

5.2 Microstructural Features

- Heavy grinding is present on the outer surface of sample V-10. Microhardness was measured as high as 383 HV near the surface indicating significant cold work at the surface. Microstructural evidence of cold work is seen to a depth of 6 to 7 mils. These surface conditions are favorable for crack initiation.
- Surface microhardness readings as high as 338 HV near the surface of sample V-9 provides evidence of cold work. Microstructural evidence of cold work was measured to a depth of about 2 mils.
- Classical weld sensitization (moderate) is seen in the weld HAZ of boat sample V-10 (crack location).
- Little evidence of sensitization is observed in boat sample V-10 for locations away from the weld HAZ.
- The degree of sensitization in the V-9 boat sample, in the location examined, is limited. There was no discernable difference between the weld HAZ and the base metal locations based upon the optical metallography.
- It was noted that the response to etching V-9 was slower than that obtained with V-10. Different etching rates are reasonable because the samples are removed from different heats of material.

5.3 Microhardness Results

- The maximum microhardness measured near the surfaces of V-10 was 383 HV and for V-9 was 338 HV. This level of hardness at the surface is consistent with the cold worked microstructures seen on the surfaces of both samples.
- Microhardness of the base material ranged from 204 to 247 HV for both plates. These values are higher than the average hardness reported for the original annealed plate material. Some degree of radiation hardening may be in evidence; however, the plates were cold formed into half cylinder shapes, and an increased base material hardness due to cold working is expected. The effect of the cold work is believed to be the primary reason for the increase in hardness over the original plate.

5.4 Chemical Composition

- The chemical composition measured in the two boat samples is consistent with the specification for Type 304 stainless steel and confirms the Certified Material Test Reports (CMTRs) for these materials.
- The carbon content was not measured, but CMTRs for the original plates indicated the carbon content was between 0.047 and 0.062 wt. % C.
- The only significant difference seen between the chemistries of the two samples was molybdenum. Sample V-10 had a Mo content of 0.19 wt. %, and sample V-9 had a Mo content of 0.33 wt. %. The presence of Mo tends to increase the tolerance of stainless steel to thermal sensitization, and this helps explain the differences in degree of sensitization between the locations examined for these two plates. [Note: Differences in rates of etching the microstructures were noted above.]

5.5 Scanning Electron Microscopy

- The intergranular nature of cracking is confirmed on the fracture face.
- Heavy (thick) oxides on the crack faces are iron oxides, likely magnetite (Fe2O3).

5.6 EPR Test Measurements

- EPR testing was completed for both boat samples
- Measurements indicate moderate sensitization in both boat samples.
- The degree of sensitization measured for sample V-10 (6 to 15 coulombs/cm^2) is slightly greater than that measured for sample V-9 (2 to 5 coulombs/cm^2) Reference 7.

5.7 Fluence Measurements

- The ID fluence at the V-9 location was measured at 3.088×10^{20} n/cm^2. The mid-wall fluence measured at the V-9 location measured 2.273×10^{20} n/cm^2.
- The mid-wall fluence measured at the V-10 location was 1.541×10^{20} n/cm^2. The OD fluence at the V-10 location measured 1.113×10^{20} n/cm2.

- The V-10 mid-wall fluence bounds the mid-wall fluence from the H-5 elevation up to the V-10 sample location.
- The ID fluence measured at the V-9 sampling location bounds the maximum fluence for both the V-9 and V-10 welds.

5.8 Tensile Testing Results

- The 550°F yield strength results of two tensile tests performed on material taken from boat sample V-9 averaged 48.1 ksi.
- The 550°F yield strength measured on material taken from boat sample V-10 was 51.0 ksi.
- The 550°F ultimate strength results of two tensile tests performed on material taken from boat sample V-9 averaged 69.75 ksi.
- The 550°F ultimate strength measured on material taken from boat sample V-10 was 74.9 ksi.
- All tensile tests were performed at 550°F.
- The testing results are consistent with that expected for Type 304 stainless steel having a fluence from 1 to 3 x 10^{20} n/cm^2.
- The tests clearly indicate that the core shroud Type 304 stainless steel material retains a high degree of ductility.

6.0 Discussion

Metallographic results clearly show the intergranular characteristics of the cracks in the V-10 sample. Cracking was initiated at a cold worked surface (ground) and propagated within the weld HAZ volume defined by thermal sensitization from welding (approximately .3 inches of the weld fusion line as measured from the V-10 sample). An increased degree of material sensitization in the volume adjacent to the weld and surrounding the crack was noted by comparing grain boundary carbide precipitation near the crack to areas away from the crack. Secondary cracks were characteristic of the cracking paths within the HAZ. These cracks generally propagated towards the weld (higher stressed position for axial stresses). Secondary cracks were completely filled with oxides indicating probable inactivity. The principal crack also had oxides on the faces of the crack, but these were fractured possibly during sample removal and metallurgical sampling. Grain encirclement by corrosion characterized the initial portion of the main crack, but was not characteristic of the deeper portions of the crack.

A team composed of representatives from General Electric Company, MPM Technologies, Altran Corporation, Niagara Mohawk, Framatome Technologies Inc., and McDermott Technology Inc reviewed the metallographic results. Results obtained for these samples were compared to results obtained from boat samples removed from cracked core shroud welds at other plants. It was concluded that the cracking is consistent with IGSCC seen elsewhere, and that surface grinding associated with fabrication produced a cold worked surface that facilitated crack initiation.

The observed characteristics are consistent with the NMP1 operating history in that during the initial 5 fuel cycles the operating conductivity was typically above 0.3 μS/cm. Figure 5 describes the average conductivity for the plant operating history. Figure 6 plots the average chloride content for the operating history. It can be seen that chloride was a major source of increased conductivity in the early years. Both average conductivity and anion content have been tightly controlled in recent years (cycle 9 to the present time) to levels consistent with the recommendations of the BWROG/EPRI Water Chemistry Guidelines, Reference 6. The pattern of significantly improved water chemistry is typical of other BWRs and signals a significantly reduced tendency for corrosion to be supported. In other words, the susceptibility to corrosion would have been much greater in the early years than it is today. Likewise crack growth rates in the recent times will be slower due to the excellent water chemistry.

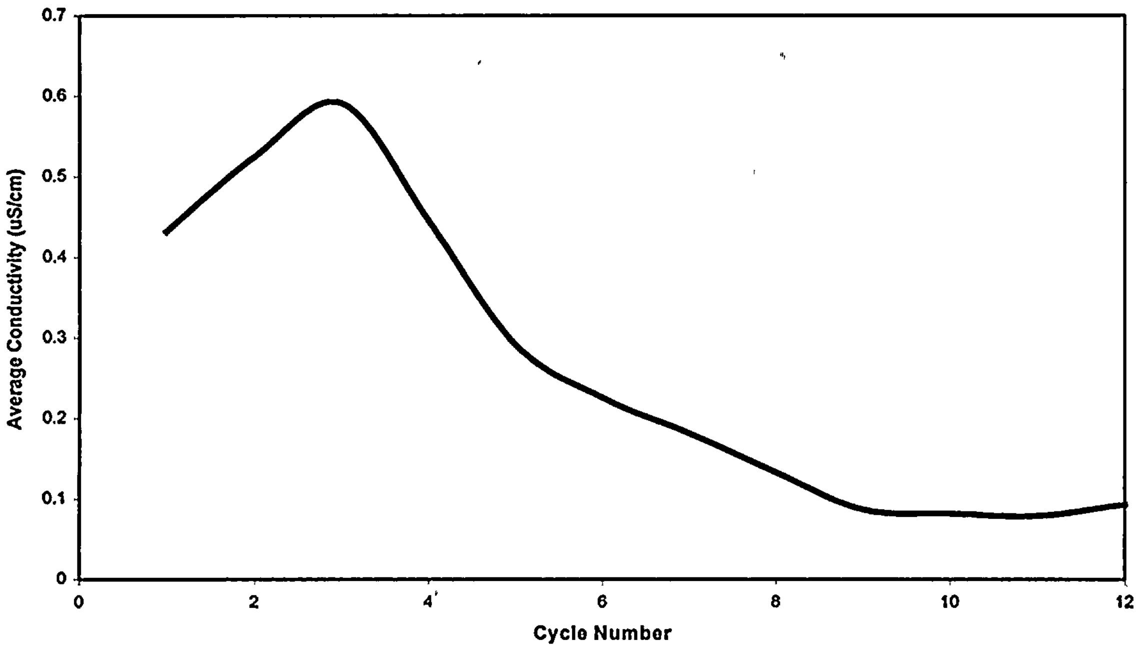

Figure 5 - Average conductivity for the first 12 cycles at NMP-1

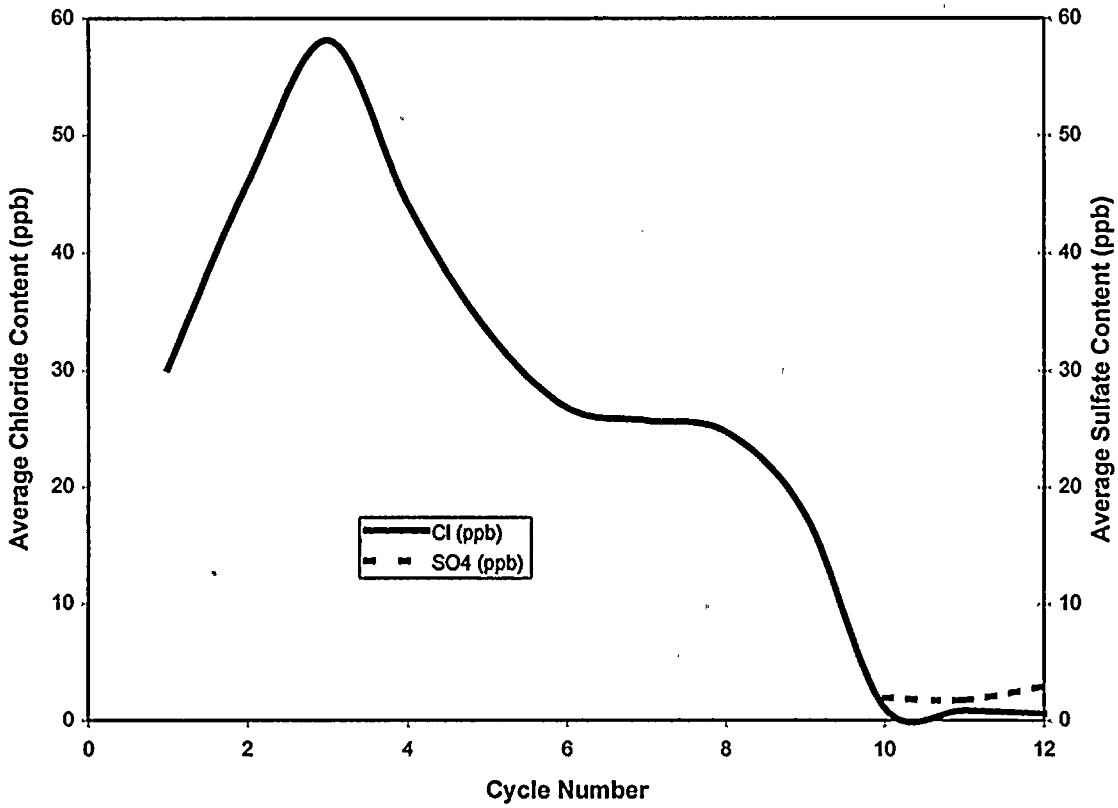

Figure 6 - Anion content for first 12 cycles at NMP-1

The crack branching, the near surface grain encirclement from corrosion processes, and the oxide filled secondary branch cracks are metallurgical features that support a cracking chronology that initiated early in the operating history of NMP1. The oxides present in the crack and the presence of oxides near the crack tip provide additional evidence supporting this chronology.

The accumulated fluence was not a significant factor in the observed cracking of the V-10 boat sample. The V-9 boat sample was not cracked and yet was exposed to a greater fluence. The peak ID fluence measured on the V-9 sample was 3.088×10^{20} n/cm^2, and V-10 mid-wall fluence measured 1.54×10^{20} n/cm^2 (Reference 9).

Miniature specimen tensile tests were performed at 550^{0}F on the V-9 boat sample material, and the results are reported in Reference 10. These results indicated that the engineering yield strength at 550^{0}F was between 45 and 50 ksi. and the tensile strength was between 68 and 71.5 ksi. The yield strength is higher and the tensile strength is lower than the respective room temperature values reported in the fabrication CMTR records (34 to 40 ksi. yield and 80 to 82 ksi. tensile strengths). Increases in yield strength are expected from two sources – cold working and irradiation. The potential sources of cold work include plate forming and fabrication. The approximately 20 ksi. difference between yield and ultimate strengths, measured for the boat sample, indicates a high degree of ductility for this material. High ductility is an

inherent property of Type 304 austenitic stainless steel, and although the differences measured at 550^0F are less than those reported for the annealed room temperature properties, the indicated ductility is excellent. The measured elongation and reduction-in-area properties confirm the excellent ductility of the boat sample material. The fluence measured at V-9 is sufficient to result in the measured increase in yield strength over the original annealed plate material. It also is noted that cold forming the plate during fabrication will introduce some degree of cold work and thus be a contributing factor. Cold forming likely will contribute to the measured increase in yield strength, unfortunately, specific data to quantify the cold work effect is not available.

The microhardness testing results were evaluated to determine the potential for irradiation hardening. The hardness of the original annealed plate material was reported in the CMTRs in terms of Brinell hardness between 149-170. These values are equivalent to microhardness values between 156-172 HV. Microhardness measurements on the bulk material of boat sample V-10 measured 220-247 HV, and similar measurements for boat sample V-9 were 204-247 HV. These values indicate a modest increase in hardness over the original annealed plate. Both cold forming and irradiation mechanisms will elevate the bulk material hardness either singly or in combination. The measured increase in hardness is likely contributed by both mechanisms, but as was the case discussed above for yield strength, specific data are unavailable with which to be definitive. The minor increase is microhardness levels is too low to have a significant influence on crack growth rates.

A large increase in hardness is seen for the material surface layers. The cold work in the surface layers likely is due to surface grinding, because the slip lines were clearly visible in the etched microstructures. Slip lines clearly delineate regions of heavy cold work. Grinding effects were seen to depths of about 5 mils in V-10 and 2 to3 mils in V-9. The microhardness measured in the surfaces from 330-380 HV on V-10 and 254-338 HV on V-9. Therefore the greatest hardness increases were measured at the surface where significant cold work was documented in the microstructures. These microhardness levels are typical of surface grinding in core shroud structures. It is known that such surfaces are significant contributors to crack initiation.

There are striking absences of metallurgical features characteristic of irradiation assisted stress corrosion cracking (IASCC) in the microstructures of the cracked sample. IASCC typically is characterized by extensive crack tip branching, grain encirclement, and grain dropout. The review team examined the cracking features developed in this evaluation and compared them to results obtained where IASCC was believed to have occurred in the core shroud of an overseas plant. The overseas plant cracking features were very different from those in the current study. All of the characteristic features of IASCC that were seen in the test sample microstructures from the overseas plant were absent from the samples examined in this study.

Second, the microstructure of the progression of cracking from the surface into the plate is instructive regarding the effects of irradiation on cracking. It was noted that grain encirclement was a feature of the main crack near the surface, but the degree to which this feature was present diminished, as the crack grew deeper. Grain encirclement is a microstructural condition identified where corrosion processes have completely separated adjacent grains. Irradiation is known to increase the degree of sensitization over time (ie. increased fluence). High levels of fluence have been associated with irradiation assisted stress corrosion (IASCC) and grain encirclement is one manifestation of IASCC. If fluence is high (e.g. $> 5\text{-}8 \times 10^{20} n/cm^2$) then grain encirclement would be expected. The fluence measured on the cracked boat sample (V-10) was

several times lower, thus the interpretation is not necessarily related to irradiation. Two key considerations are important - 1) fluence is time dependent and increases with time, and 2) the crack is propagating into material that must be at a higher fluence (higher flux) and cracking occurs over time. Both of these factors would suggest increased grain encirclement towards the tip of the crack, grain dropout, and increased branching. However, none of these characteristics were observed; therefore it is deduced that irradiation was not a significant factor for either initiation or propagation of the vertical weld cracking.

Third, EPR test results were measured on the cross-sections of both boat samples using the double loop field technique (Reference 8). These results indicated that the electrochemical current generated from active grain boundaries is moderate for both boat samples. The measurements were consistent with measurements expected for normal weld sensitization produced by thermal mechanisms associated with welding. The V-9 boat sample was removed from a location expected to have a maximum fluence for the core shroud materials. The EPR measured on this sample was 2 to 5 coulombs/cm^2. These values were slightly lower than the EPR test results measured for the V-10 boat sample that was cracked (5 to 15 coulombs/cm^2). The V-10 boat sample was at a lower fluence, because it was removed from the outer surface of the shroud at an elevation slightly below the core mid-plane. The EPR results were corroborated by the metallographic results. The etching characteristics of the microstructures in the two samples suggested that both boat samples were moderately sensitized, but the degree of sensitization seen in boat sample V-10 was slightly greater than was seen in boat sample V-9. These observations would have been reversed if significant radiation induced sensitization had taken place. These findings provide no evidence to support accelerated cracking due to irradiation effects (IASCC). Therefore, it was concluded that normal IGSCC processes controlled the cracking observed in the vertical welds.

7.0 Conclusions

The metallurgical results of this examination provide confirming evidence that the cracking seen is the result of intergranular stress corrosion cracking (IGSCC) similar to that experienced in other BWR components exposed to the oxidizing environment of the BWR.

There is no evidence that irradiation (neutron flux) has degraded grain boundaries either through irradiation induced chromium depletion or through impurity element segregation. No metallurgical features, uniquely characteristic of IASCC were observed, and it was concluded that IASCC was not a factor in the vertical weld cracking at NMP1. Results from EPR testing suggested that the role of irradiation was minimal. In addition, the range of fluence measured in the boat samples was low (1×10^{20} n/cm^2 to 3×10^{20} n/cm^2) (Reference 9). Therefore increased corrosion susceptibility from irradiation induced changes in grain boundary composition is not supported.

Crack initiation was enhanced on the outside surfaces adjacent to the vertical welds because the surfaces were heavily ground, creating conditions favorable for crack initiation. The level of sensitization observed in the HAZ is consistent with thermal sensitization expected for welded 304 SS having these carbon levels. The level of sensitization estimated from the results of optical metallography (Reference 5), and measured using EPR techniques (Reference 8) for the boat samples are consistent with the assumed degree of sensitization (DOS) used in the PLEDGE analysis to predict cracking behavior (References 1 and 7).

Therefore, the DOS assumptions used in the PLEDGE crack growth analysis were appropriate. These findings have been confirmed by GE Nuclear Energy based upon their technical review of project results.

The crack depth measured in the V-10 boat sample is consistent with the ultrasonic depth measurements performed adjacent to the location from which the boat sample was removed. The crack depths measured on the V-10 boat sample were consistent at all locations along the length of the sample.

These results indicate that assumptions regarding the levels of material sensitization, the role of cold worked surfaces enhancing crack initiation, and the predicted rates of crack propagation using radiolysis modeling were conservative. These findings confirm that cracking identified in the NMP-1 core shroud vertical welds is consistent with the mechanistic understanding for IGSCC initiation and growth processes for BWR core shrouds as described in BWRVIP-14. The combined boat sampling testing program results prove that the NMP-1 core shroud material condition is consistent with and bounded by the basis for the BWRVIP-14 disposition crack growth rate of 2.2×10^{-5} inches/hour.

8.0 References

1. General Electric Nuclear Energy (GENE), "Assessment of the Vertical Weld Cracking on the NMP1 Shroud", GENE-523-B13-01869-043.
2. MPM Technologies, "Analysis of Nine Mile Point Unit 1 Shroud Welds V9 and Weld V10 Cracking", Report No. MPM-497439, April 1997.
3. Altran Corporation, "Nine Mile Point Unit 1 Core Shroud Cracking Evaluation", letter report from Richard E. Smith to George Inch dated April 3, 1997.
4. NRC Safety Evaluation Report dated May 8, 1997, regarding the results of the reinspection of the core shroud for Nine Mile Point 1.
5. McDermott Technology Inc., "Niagara Mohawk's Nine Mile Point Unit 1 Boat Samples Analyses - Part 1: Metallography", RDD:98:55863-002-000:01, September 1997.
6. BWR Water Chemistry Guidelines- 1993 Revision – Normal and Hydrogen Water Chemistry, prepared by BWROG Water Chemistry Guidelines Revision Committee, EPRI TR-103515, Project 2493 – Final Report, February 1994.
7. General Electric Nuclear Energy (GENE), "Assessment of Crack Growth Rates Applicable to Nine Mile Point-1 Vertical Weld Indications", GE-NE-523-B13-01869-113, Rev. 0, February 1998.
8. Altran Corporation, "EPR Testing of Boat Samples from Core Shroud Vertical Welds V-9 and V-10 at NMP-1", Technical Report No. 97181-TR-03-Rev. 0, February 1998.
9. Framatome Analysis Report: 86-1266298-00, "Fluence Analysis Report for Boat Samples – Nine Mile Pt. 1", January 28, 1998.
10. McDermott Technology Inc., "Niagara Mohawk's Nine Mile Point Unit 1 Boat Samples Analyses - Part III: Tension Tests", RDD:98:55863-004-000:01, February 1998.
11. Altran Corporation, "Evaluation of Metallurgical Analyses of Core Shroud Vertical Weld Boat Samples from Nine Mile Point Unit 1", Technical Report No. 97181-TR-01, Rev. 1, September 1997.

6